Available online at www.sciencedirect.com
ScienceDirect
C. R. Chimie 11 (2008) 398–406
COMPTES RENDUS CHIMIE
http://france.elsevier.com/direct/CRAS2C/

Full paper / Mémoire

Calcium phosphates: First-principles calculations vs. solid-state NMR experiments

Frédérique Pourpoint [a], Christel Gervais [a], Laure Bonhomme-Coury [a], Francesco Mauri [b], Bruno Alonso [c], Christian Bonhomme [a,*]

[a] *Université Pierre-et-Marie-Curie–Paris-6, UMR 7574 CNRS, Laboratoire de chimie de la matière condensée de Paris, 4, place Jussieu, Paris F-75005, France*
[b] *Université Pierre-et-Marie-Curie–Paris-6, UMR 7590 CNRS, Laboratoire de minéralogie–cristallographie de Paris, Paris F-75005, France*
[c] *Institut Charles-Gerardt, UMR 5223 CNRS–UM2–ENSCM–UM1, MACS, 8, rue de l'École-Normale, Montpellier F-34000, France*

Received 29 April 2007; accepted after revision 28 September 2007
Available online 26 December 2007

Abstract

Calcium phosphates (including hydroxyapatite) are inorganic components of numerous compounds such as bones and teeth. The in-depth characterization of their structures is of crucial importance for the understanding of the properties of biocompatible materials. Multinuclear solid-state NMR (including ^{1}H, ^{17}O and ^{31}P) appears as a valuable tool of investigation. In this paper, we show that full assignments of spectra were obtained through extensive use of first-principles calculations, based on the GIPAW (Gauge Included Projector Augmented Wave) approach [C.J. Pickard, F. Mauri, Phys. Rev. B 63 (2001) 245101]. ^{1}H and ^{31}P calculations (isotropic chemical shifts and CSA tensors) were validated by comparison with MAS experiments. In the case of ^{1}H, full resolution was not obtained and subsequent assignment of resonances was obtained by taking into account the calculated isotropic chemical shifts. Interesting correlations involving δ_{iso} (^{1}H) values and H-bond networks (characterized by internuclear distances) were established, in good agreement with empirical data already published in the literature. ^{1}H CSA tensors were also analyzed. Furthermore, ^{17}O is a suitable spectroscopic target for the characterization of X–O–Y bonds, which may be present at bioinorganic interfaces. First-principles calculations showed that PO^{-}, P–O–P, POH, CaO (and H_2O) entities could be distinguished on the basis of ^{17}O chemical shifts and quadrupolar constants in MQ-MAS experiments. ***To cite this article: F. Pourpoint et al., C. R. Chimie 11 (2008).***

Résumé

Les phosphates de calcium (et les hydroxyapatites) sont des composants inorganiques présents dans de nombreux composés biologiques, tels que les os et les dents. La caractérisation détaillée de leurs structures est nécessaire à la compréhension des propriétés des matériaux biocompatibles. Dans ce cadre, la RMN multinucléaire à l'état solide (^{1}H, ^{17}O et ^{31}P) apparaît comme une technique de caractérisation de choix. Dans cet article, nous montrons que l'attribution complète des spectres peut être obtenue à l'aide de méthodes quantiques fondées sur l'approche GIPAW (*Gauge Included Projector Augmented Wave*) développée initialement par Mauri et Pickard [C.J. Pickard, F. Mauri, Phys. Rev. B 63 (2001) 245101]. Les calculs de déplacements chimiques isotropes ^{1}H et ^{31}P, ainsi que de tenseurs CSA, sont validés par comparaison avec des expériences MAS. Dans le cas du

* Corresponding author.
E-mail address: bonhomme@ccr.jussieu.fr (C. Bonhomme).

1631-0748/$ - see front matter © 2007 Académie des sciences. Published by Elsevier Masson SAS. All rights reserved.
doi:10.1016/j.crci.2007.09.011

proton, la résolution ultime des spectres n'est pas atteinte et l'interprétation des spectres a été rendue possible par l'utilisation des calculs GIPAW relatifs aux déplacements chimiques isotropes. D'intéressantes corrélations entre les valeurs de δ_{iso} (^{1}H) et les réseaux de liaisons H (décrits en terme de distances internucléaires) sont mises en évidence, corroborant des données empiriques publiées dans la littérature. Les tenseurs CSA ^{1}H ont été également analysés. De plus, l'oxygène 17 est une cible spectroscopique potentielle pour la caractérisation de liaisons X–O–Y (celles-ci pouvant être présentes au niveau des interfaces bioinorganiques). Les calculs GIPAW montrent que les groupements PO^-, P–O–P, POH, CaO (et H_2O) peuvent être distingués via leurs déplacements chimiques et leurs constantes quadripolaires dans des expériences MQ-MAS. ***Pour citer cet article : F. Pourpoint et al., C. R. Chimie 11 (2008).***

Keywords: First-principles calculations; Calcium phosphates; ^{31}P CSA tensors; ^{1}H CSA tensors

Mots-clés : Calculs ab initio ; Phosphates de calcium ; Tenseurs CSA ^{31}P ; Tenseurs CSA ^{1}H

1. Introduction

Calcium phosphates have been widely studied for dentistry and orthopedic implants because of their high biocompatibility and bioresorbability [1–3]. Hydroxyapatite derivatives ($Ca_5(PO_4)_3(OH)$) (including carbonated apatitic phases) give bones, teeth and tendons their hardness and stability. By "playing" with the chemical composition, selective protein adsorption properties can be obtained for nanocrystalline hydroxyapatite [4]. Apatitic materials may also act as drug delivery systems [5–8].

Solid-state NMR is definitely suitable for the in-depth characterization of calcium phosphate phases. ^{31}P NMR has been largely used in the past, in combination with $^1H \rightarrow {}^{31}P$ Cross-Polarization transfer [9]. Moreover, inorganic components in bones were investigated [10]. ^{1}H solid-state NMR has been rarely used [11] due to the lack of resolution related to the strong homogeneous $^1H–{}^1H$ dipolar interaction. Multiple pulses experiments combined with MAS (CRAMPS) [12] have been implemented for the characterization of calcium phosphate phases [13]. Nevertheless, full assignment of proton lines remains difficult, though empirical trends correlating the isotropic chemical shifts and the H-bond networks have been proposed in the literature some decades ago [14]. In this paper, we demonstrate that first-principles calculations are validated for ^{31}P solid-state NMR. Calculated CSA tensors are in very good agreement with experimental data obtained by MAS or static experiments. When considering ^{1}H MAS spectra (at very high field and very fast rotation frequency), calculated data become essential for full assignment of the experimental spectra. All calculations were done by using the GIPAW method first developed by Mauri and Pickard (see Section 2) [15].

^{17}O solid-state NMR experiments appear as a straightforward tool of characterization of the local structure of inorganic materials [16] by probing directly and quantifying the different types of oxo-bridges present in the structure. The ^{17}O isotropic chemical shift values of M–O–M′ fragments (M, M′ = Si, P, Ti, Zr,…) are indeed highly sensitive to the chemical nature of M and M′ [17–19]. However, the main drawback of this technique is its poor sensitivity, due to the low natural abundance of the ^{17}O isotope (0.037%). In the field of phosphate compounds, this problem can nonetheless be overcome either by using ^{17}O-enriched water for the hydrolysis step of the precursors [20] or by heating the final material under ^{17}O-enriched water vapour [21] or $^{17}O_2$ gas [22]. Despite isotopic enrichment and high-resolution MQ-MAS (Multiple-Quantum Magic-Angle Spinning [23]) methods, the interpretation of ^{17}O spectra still remains difficult, as no empirical rules have yet been found to enable the assignment of the peaks and to obtain structural information for each site. In this context, first-principles calculations can be particularly useful in the understanding of spectra, since accurate calculation of the NMR parameters will allow the assignment of all sites.

^{43}Ca ($I = 7/2$, 0.145%) NMR remains exotic in inorganic chemistry due to very low sensitivity and large quadrupole moment. It must be noticed that recent work dealing with model compounds and ^{43}Ca NMR characterization at high field has been carried out in the literature by using large amount of samples [24].

The outline of the article is the following: Section 2 presents the syntheses of the studied calcium phosphate phases, including protonated structures ($CaHPO_4 \cdot 2H_2O$, Brushite and $Ca(H_2PO_4)_2 \cdot H_2O$, MCPM) and non-protonated structures (β-$Ca(PO_3)_2$ and $Ca_4P_2O_9$, TTCP). The first-principles calculations and the GIPAW approach are also described in Section 2. Section 3 deals with results and discussion: the calculated and experimental ^{31}P are first discussed for all structures, including polymorphs of $Ca(PO_3)_2$. ^{1}H NMR

data are discussed for protonated phases, emphasizing the calculation of CSA tensors and the strong influence of H bonding. Finally, ^{17}O predicted data (isotropic chemical shifts and quadrupolar constants) are summarized and discussed.

2. Experimental

Brushite, $CaHPO_4 \cdot 2H_2O$ (Fig. 1), was synthesized by mixing calcium carbonate and H_3PO_4 (85%) in water (Ca/P = 1). The mixture was stirred at room temperature until precipitation. For Ca/P = 0.5, MCPM, $Ca(H_2PO_4)_2 \cdot H_2O$ (Fig. 2), was obtained. By heating MCPM at 600 °C (10 h), β-$Ca(PO_3)_2$ (Fig. 3) was synthesized. TTCP, $Ca_4P_2O_9$ (Fig. 4), was obtained by mixing calcium carbonate and monetite ($CaHPO_4$) at 1400 °C for 10 h, followed by quenching in air. The obtained compounds were systematically checked by powder X-ray diffraction (Brushite, JCPDS: 72-1240; MCPM, JCPDS: 70-0090; β-$Ca(PO_3)_2$, JCPDS: 11-0039; TTCP, JCPDS: 70-1379).

^1H NMR experiments were recorded on a Bruker AVANCE 750 spectrometer in order to enhance resolution (^1H: 750.16 MHz). A zirconia rotor (2.5 mm) was spun at 33 kHz at the magic angle. The number of scans

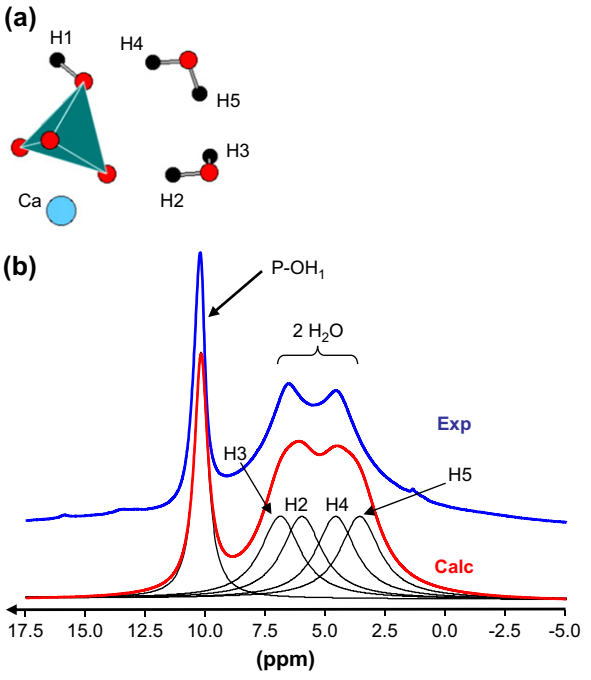

Fig. 1. (a) Schematic representation of atoms involved in brushite. (b) ^1H MAS NMR spectra (experimental and calculated) of brushite (17.6 T, 34 kHz). The calculated spectrum is obtained by using the GIPAW values given in Table 1.

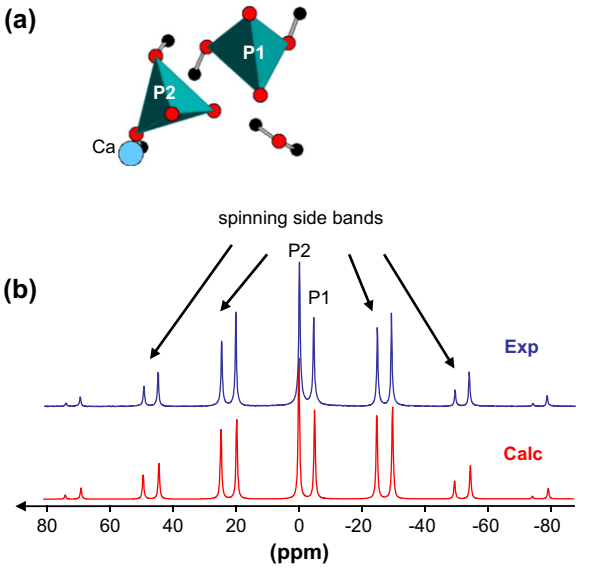

Fig. 2. (a) Schematic representation of atoms involved in MCPM. (b) ^{31}P MAS NMR spectra (experimental and calculated) of MCPM (7 T, 3 kHz).

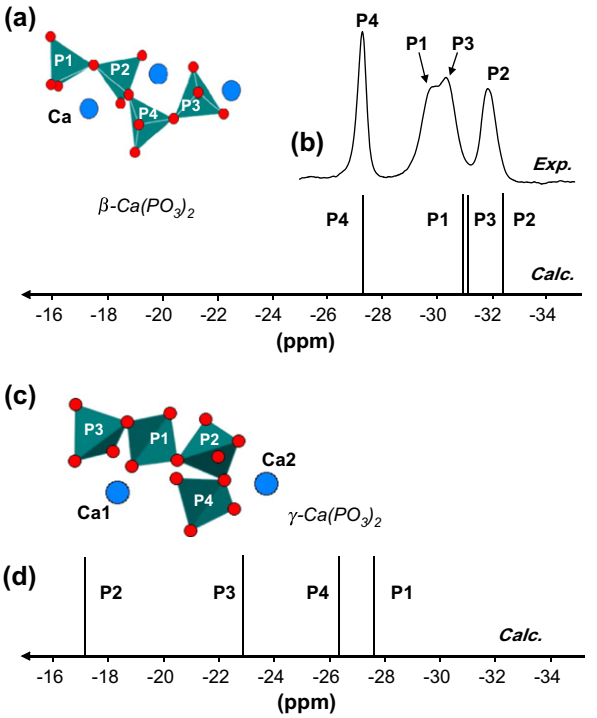

Fig. 3. (a) Schematic representation of atoms involved in β-$Ca(PO_3)_2$. (b) ^{31}P MAS NMR spectra (experimental and calculated) of β-$Ca(PO_3)_2$ (7 T, 14 kHz). (c) Schematic representation of atoms involved in γ-$Ca(PO_3)_2$. (d) ^{31}P MAS NMR spectrum (calculated) of γ-$Ca(PO_3)_2$ (7 T, 14 kHz).

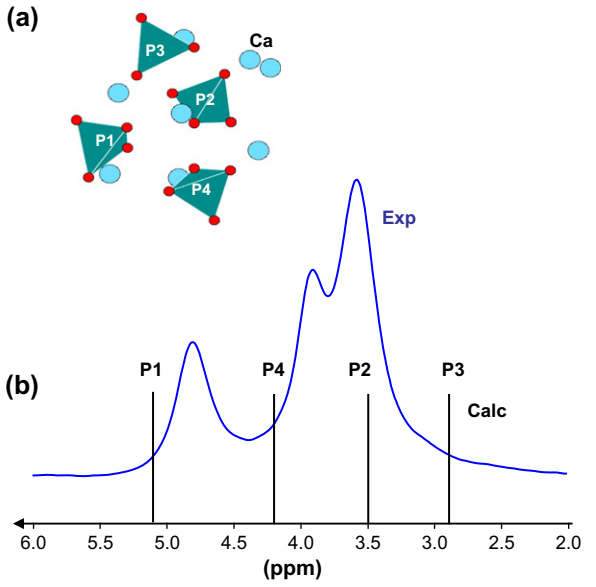

Fig. 4. (a) Schematic representation of atoms involved in TTCP. (b) ^{31}P MAS NMR spectra (experimental and calculated) of TTCP (7 T, 14 kHz).

(NS) was 4, the pulse length was 1.7 μs (30°), and the relaxation delay (RD) was 30 s. The spectra were referenced to TMS. ^{31}P MAS NMR experiments were performed on a Bruker AVANCE 300 (^{31}P: 121.44 MHz) using a 4-mm Bruker probe under ^{1}H high power decoupling (TPPM pulse sequence) (pulse length: 1.6 μs (30°), RD: 30 s). Spectra were referenced to H_3PO_4 (85%). A zirconia rotor (4 mm) was spun at 3 and 14 kHz.

The first-principles calculations were performed within the Kohn–Sham DFT. The PBE generalized gradient approximation [25] was used and the valence electrons were described by norm-conserving pseudopotentials [26] in the Kleinman–Bylander [27] form. The core definition for O is $1s^2$ and it is $1s^22s^22p^6$ for P and Ca. The core radii are 1.2 a.u. for H, 1.5 a.u. for O and 2.0 a.u. for P and Ca. The wave functions are expanded on a plane wave basis set with a kinetic energy cut-off of 80 Ry. The crystalline structure is described as an infinite periodic system using periodic boundary conditions. The NMR calculations were performed for the experimental geometries determined by neutron or X-ray diffraction for the various calcium phosphates: brushite, $CaHPO_4\cdot 2H_2O$ [28]; MCPM, $Ca(H_2PO_4)_2\cdot H_2O$ [29]; β-$Ca(PO_3)_2$ [30]; γ-$Ca(PO_3)_2$ [31]; $Ca_4P_2O_9$ [32]. In the case of $Ca_4P_2O_9$, a significant better agreement is obtained between experimental and calculated ^{31}P parameters by taking into account a geometry optimization (starting from the experimental geometry and allowing the positions of the atoms to relax using DFT calculations). The new coordinates obtained after relaxation are summarized in Supporting information. The integral over the first Brillouin zone was performed using a Monkhorst–Pack $2\times2\times2$ k-point grid [33] for the charge density and electric-field gradient calculation and a $4\times4\times4$ k-point grid for the chemical shift tensor calculation. The calculations have been performed at the IDRIS supercomputer centre of the CNRS using a parallel IBM Power4 (1.3 GHz) computer; the calculation of the Electric Field Gradient (EFG) and CSA tensors requires from 2 to 10 h on 32 processors. The shielding tensor is computed using the GIPAW approach which permits the reproduction of the results of a fully converged all-electron calculation, while the EFG tensors are computed using a PAW approach. The isotropic chemical shift δ_{iso} is defined as $\delta_{iso} = -[\sigma - \sigma^{ref}]$ where σ is the isotropic shielding and σ^{ref} is the isotropic shielding of the same nucleus in a reference system. In our calculations, absolute shielding tensors are obtained. The σ^{ref} values were chosen by comparison between experimental and calculated δ_{iso} in a series of SiO_2 polymorphs [34a] for ^{17}O and other organophosphorus derivatives for ^{1}H and ^{31}P: σ^{ref} (^{17}O) = 261.5 ppm, σ^{ref} (^{1}H) = 31.0 ppm, and σ^{ref} (^{31}P) = 300.7 ppm. Diagonalisation of the symmetrical part of the calculated shielding tensor provides its principle components δ_{11}, δ_{22} and δ_{33} defined such as $|\delta_{33} - \delta_{iso}| \geq |\delta_{11} - \delta_{iso}| \geq |\delta_{22} - \delta_{iso}|$ and $\delta_{iso} = 1/3(\delta_{11} + \delta_{22} + \delta_{33})$. Similarly, the principle components V_{xx}, V_{yy}, and V_{zz} of the EFG tensor defined as $|V_{zz}| \geq |V_{xx}| \geq |V_{yy}|$ are obtained by diagonalisation. The quadrupolar interaction can then be characterized by the quadrupolar coupling constant C_Q (with its sign) and the asymmetry parameter η_Q defined as: $C_Q = eQV_{zz}/h$ and $\eta_Q = (V_{yy} - V_{xx})/V_{zz}$. It has to be noticed that the role of Ca–O bonds within the frame of GIPAW calculations has been carefully studied by Profeta et al. [34b]. It was demonstrated that an easy and transferable correction of the PBE–DFT theory was possible for the accurate calculations of NMR parameters.

3. Results and discussion

3.1. ^{31}P: calculated vs. experimental data

Brushite, $CaHPO_4\cdot 2H_2O$, is characterized by a unique P crystallographic site (Fig. 1a). Static experiments (not shown here) allowed to extract the three principle components of the ^{31}P CSA tensor (Table 1). Experimental and GIPAW calculated values are in very good agreement for all components. In the case

Table 1
Calculated ^{1}H, ^{17}O and ^{31}P NMR parameters for brushite $CaHPO_4 \cdot 2H_2O$, MCPM $Ca(H_2PO_4)_2 \cdot H_2O$, β-$Ca(PO_3)_2$, γ-$Ca(PO_3)_2$, and $Ca_4P_2O_9$

	δ_{iso} (ppm)		C_Q (MHz)	η_Q	δ_{11} (ppm)	δ_{22} (ppm)	δ_{33} (ppm)
	Calc	Exp	Calc	Calc	Calc (exp)	Calc (exp)	Calc (exp)
Brushite							
P1	2.0	1.6			−59.7 (−54.2)	−3.5 (−5.6)	69.1 (64.7)
H1 (POH)	10.2				19.9	18.1	−7.4
H2 (H_2O)	6.0				15.9	15.2	−13.0
H3 (H_2O)	6.9				17.0	15.7	−12.0
H4 (H_2O)	4.6				14.1	13.1	−13.3
H5 (H_2O)	3.5				11.6	9.3	−10.3
O (POH)	75.5		6.9	0.9			
O (PO···Ca)	100.9–116.6		4.6–4.8	0.0–0.3			
O (H_2O)	−11.0 and −21.1		7.7 and 9.0	0.8 and 0.9			
MCPM							
P1	−4.1	−4.2			−71.0 (−73.4)	−7.0 (−4.2)	66.0 (65.0)
P2	0.8	0.3			−50.0 (−51.2)	−4.0 (−2.3)	55.5 (54.4)
H1 (POH)	12.2				24.0	22.4	−9.9
H2 (POH)	10.4				22.2	19.8	−10.7
H3 (POH)	8.8				19.4	17.2	−10.2
H4 (POH)	9.9				21.3	19.6	−11.1
H5 (H_2O)	6.4				16.9	14.8	−12.6
H6 (H_2O)	5.1				11.9	11.1	−7.7
O (PO···Ca)	91.4–99.4		4.5–4.7	0–0.1			
O (POH)	64.5–74.9		6.7–7.5	0.7–0.8			
O (H_2O)	−0.9		7.6	0.8			
β-$Ca(PO_3)_2$							
P1	−30.8	−29.9			67.8 (61.3)	3.5 (−3.4)	−163.9 (−147.4)
P2	−32.3	−31.8			66.6 (58.9)	10.1 (2.5)	−173.7 (−157.0)
P3	−30.9	−30.3			65.4 (60.8)	−3.2 (−3.9)	−155.0 (−148.0)
P4	−27.3	−27.3			57.2 (52.7)	−2.6 (−7.3)	−136.4 (−127.4)
O (PO···Ca)	97.4–117.3		4.4–4.8	0.1–0.3			
O (POP)	100.1–118.2		8.1–8.3	0.2–0.4			
γ-$Ca(PO_3)_2$							
P1	−29.3				74.1	9.9	−172.0
P2	−17.2				68.6	11.3	−131.5
P3	−22.7				75.2	11.8	−155.1
P4	−26.3				78.1	10.1	−167.2
O (PO···Ca)	91.8–109.3		4.5–5.0	0.1–0.3			
O (POP)	102.7–130.3		7.6–7.9	0.4–0.5			
$Ca_4P_2O_9$							
P1	5.1				22.1	6.2	−12.7
P2	3.5				24.5	9.9	−23.8
P3	2.9				15.4	11.2	−17.8
P4	4.2				−4.2	0.8	16.3
O (PO···Ca)	108.7–158.7		4.1–6.0	0.1–0.3			
O (Ca···O)	294.7–306.8		0.7–0.9	0.1–0.8			

^{31}P experimental CSA tensor components are also reported for brushite, $Ca(H_2PO_4)_2 \cdot H_2O$ and β-$Ca(PO_3)_2$.

of MCPM, two P sites are involved (Fig. 2a). The corresponding low-frequency ^{31}P MAS NMR spectrum (at 3 kHz) is presented in Fig. 2b. The calculated spectrum is again in very good agreement, when considering both the ^{31}P isotropic chemical shifts and the full CSA data (Table 1). The experimental CSA is characterized by the relative intensities of the spinning sidebands and can be extracted by using the DMFit program [35]. The two isotropic chemical shifts are separated by ∼5 ppm. This difference seems sufficient for safe assignment of the resonances: P1 corresponds therefore to the most shielded resonance.

The structure of β-$Ca(PO_3)_2$ is presented in Fig. 3a. It contains chains of cornerlinked phosphate groups running in an unidirectional manner through the structure. Four P crystallographic sites are involved and four resonances are indeed observed in the corresponding ^{31}P MAS NMR spectrum (Fig. 3b). The chemical shift difference between the less and most shielded resonances is ∼5 ppm. These resonances are consequently assigned to P2 and P4, respectively (Table 1). The assignment of the remaining resonances (P1 and P3) has been achieved by combining calculated data and ^{31}P/^{31}P MAS-*J*-INADEQUATE [36a] experiments [37]. Recently [31], a new polymorph of $Ca(PO_3)_2$ (namely γ-$Ca(PO_3)_2$) has been described in the literature. Chains of cornerlinked phosphate groups are also present, exhibiting different geometries when compared to the β-$Ca(PO_3)_2$ chains (Fig. 3c). The calculated ^{31}P isotropic chemical shifts are obviously deshielded when compared to β-$Ca(PO_3)_2$ (Fig. 3d). Such results are in good agreement with ^{31}P experimental data presented in Ref. [31].

The results obtained for brushite, MCPM, β- and γ-$Ca(PO_3)_2$ tend to validate the GIPAW calculations of ^{31}P CSA parameters. The ^{31}P MAS NMR spectrum of TTCP (Fig. 4b) shows overlapping isotropic resonances in a range less than 2 ppm. The four calculated lines (corresponding to the four P crystallographic sites — Fig. 4a) lie obviously in the same range. At this stage, it seems impossible to assign safely each line. As monophosphate groups are involved, experiments involving ^{31}P/^{31}P dipolar recoupling [36b] should help for full assignment of the MAS spectrum.

3.2. ^{1}H: calculated vs. experimental data

Ab initio calculations of ^{1}H parameters are rarely described [38]. In most cases, ^{1}H data are calculated within the cluster approximation [39], with some exceptions involving mainly organic molecules [40]. Only δ_{iso} (^{1}H) values are discussed. It should be noticed that empirical correlations involving the δ_{iso} (^{1}H) values and the internuclear distances have been previously described in the literature [14]. The goal of this section is to revisit such correlations from the first-principles calculation point of view.

Fig. 1b presents the ^{1}H MAS NMR spectrum of brushite obtained at very high field ($B_0 = 17.6$ T) and very fast rotation frequency (up to 34 kHz). Full resolution is not attained due to the strong ^{1}H/^{1}H dipolar interaction, which is homogeneous in nature [41]. However, three resonances located at ∼4.0, 6.5 and 10.0 ppm are observed. Calculated GIPAW values are summarized in Table 1, leading to the calculated spectrum shown in Fig. 1b. The most deshielded line corresponds obviously to PO*H* groups. The other resonances are safely assigned to protons belonging to water molecules. In a sense, calculations allowed full assignment and interpretation of the MAS spectrum. Calculated ^{1}H data related to MCPM are also given in Table 1.

Fig. 5 presents all calculated δ_{iso} (^{1}H) values vs. the shortest O*H*···*O* distances (extracted mainly from neutron diffraction data). Distinct ranges for H_2O and PO*H* resonances are evidenced. Moreover, for a given range, deshielding of protons associated with a shortening of the O*H*···*O* distances is clearly demonstrated. Recently [42], such results have been extended to ^{1}H data related to phenylphosphonic and phenylphosphinic acids. The ^{1}H CSA data shown in Table 1 are consistent with nearly axial symmetry for all tensors (H_2O and PO*H*). Such data are in agreement with results already published in the literature [43]. Nevertheless, Wu et al. [44] have pointed out that ^{1}H CSA tensors could deviate

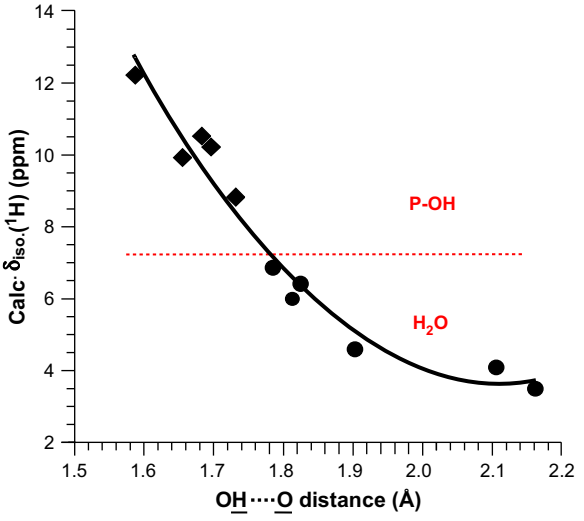

Fig. 5. Correlation between the *calculated* ^{1}H isotropic chemical shifts and the shortest internuclear distances for Brushite and MCPM.

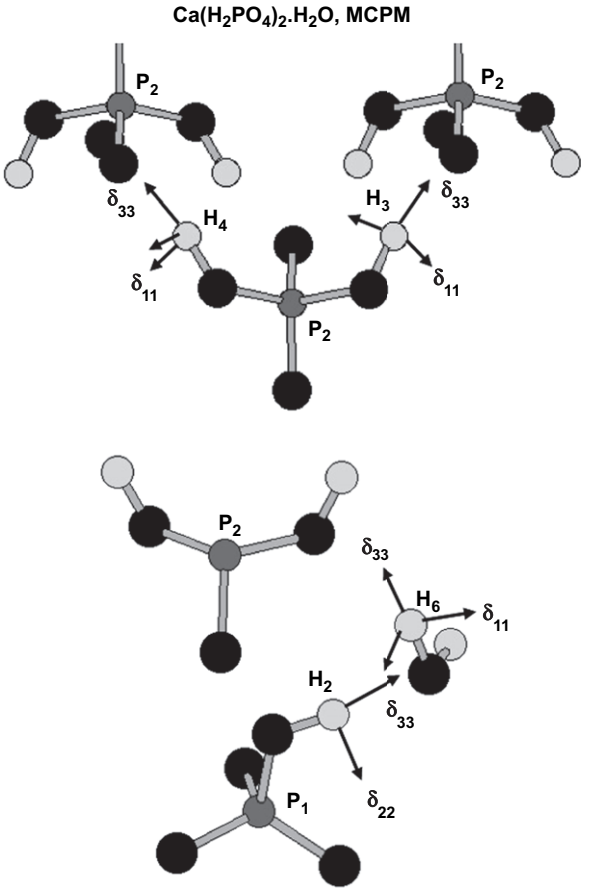

Fig. 6. Absolute orientations of ^{1}H tensors for MCPM (PO*H* and H_2O).

from axial symmetry in the case of crystalline hydrates (involving perchlorate and sulphate derivatives). Fig. 6 presents the absolute orientations of ^{1}H CSA tensors in the case of MCPM. For PO*H* and H_2O protons, the unique axis (δ_{33}) of the CSA tensors is nearly collinear to the OH···O bond direction.

3.3. ^{17}O: calculated data

In the field of calcium phosphates, few ^{17}O NMR results have been published until now to our knowledge. Only ^{17}O MAS NMR spectra of Brushite and hydroxyapatite were previously reported [45].

The aim of the calculation of ^{17}O NMR parameters in the various compounds presented in this paper is to determine whether there is a possibility to distinguish clearly the various types of oxygen environments present in calcium phosphates (Ca···O, P–O···Ca, P–O–P, P–OH and H_2O) by using ^{17}O NMR spectroscopy. The results are summarized in Table 1. The previously reported ^{17}O NMR values for P–O–P sites in h-P_2O_5 [22], Ca···O in lime [46] (CaO) and P–O···Ca environments in brushite and HAp45 are in very good agreement with the ones obtained by the calculations. Moreover, it should be noticed that the relatively large ^{17}O quadrupolar coupling constants calculated for water molecules in brushite and MCPM compare well with those experimentally observed in *p*-toluenesulphonic acid hydrate [47] and oxalic acid dihydrate [48]. Similarly, the ^{17}O P–OH parameters are consistent with those measured in phenylphosphonic [49] and phenylphosphinic [42] acid.

Ca···O environments are expected in a very distinct area with high chemical shift values (around 300 ppm) and very small quadrupolar coupling constants (less than 1 MHz). Similarly H_2O sites are well separated with small chemical shift values ($\leq$0 ppm) and very large quadrupolar coupling constants (>7.5 MHz). On the other hand, P–O···Ca, P–O–P and P–OH environments appear in the same chemical shift range (between 65 and 115 ppm). To evaluate which type of oxygen environment can be clearly distinguished experimentally, we have calculated the ^{17}O 3QMAS spectrum corresponding to the different oxygen sites (Fig. 7) [50]. Each ^{17}O site gives rise to a sharp resonance in the δ_{3Qiso} dimension at the position:

$$\delta_{3Qiso} = -17/31\delta_{iso} + 10/31\delta_{iso}^{2Q}$$

and a broad MAS spectrum in the MAS dimension with a centre of gravity given by:

$$\delta_{3QMAS} = \delta_{iso} + \delta_{iso}^{2Q}$$

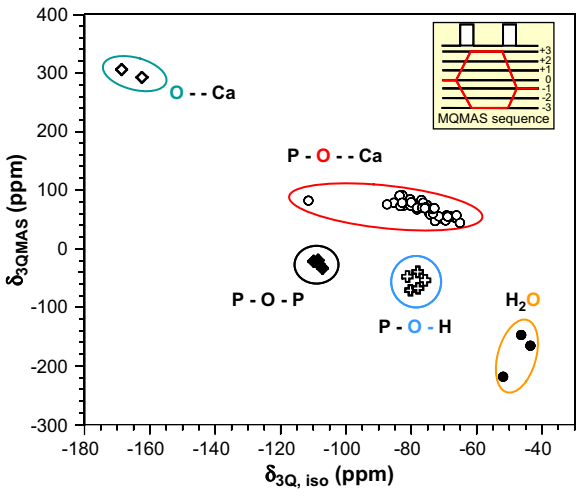

Fig. 7. Theoretical positions of various ^{17}O sites present in calcium phosphate phases in a ^{17}O 3QMAS NMR experiment ($B_0 = 9.4$ T).

where δ_{iso} is the isotropic chemical shift and δ_{iso}^{2Q} the second-order quadrupolar shift given for $I = 5/2$ by $6000P_Q^2\omega_0^2$, with ω_0 the Larmor frequency and $P_Q = C_Q(1 + \eta_Q^2/3)^{1/2}$.

The 2D spectrum shows that all types of oxygen environments investigated in this study appear in relatively distinct areas and should therefore be distinguishable using the 3QMAS NMR sequence. Indeed, even if P–O···Ca, P–O–P and P–OH environments have similar isotropic ^{17}O chemical shifts, the discrimination is possible, thanks to different C_Q values.

It can be noticed that the ^{17}O chemical shift range observed for P–O···Ca environments is rather large and it was suggested that the shifts could discriminate between different P–O bond lengths in PO_4^{3-} units [45]. Calculations show indeed that δ_{iso} (^{17}O) tends to increase with $P–O\cdots$Ca bond length.

4. Conclusions

It has been shown that first-principles calculations (using the GIPAW approach) are suitable for the interpretation of multinuclear solid-state NMR spectra of calcium phosphate phases, even in the case of non-fully resolved ^1H MAS experiments. Full tensor data are obtained for ^1H and ^{31}P, including the absolute orientation of the principle axes. Interesting correlations between the δ_{iso} (^1H) values and the shortest $OH\cdots O$ distances have been established, giving a more theoretical background to empirical data already published in the literature. Calculated ^{17}O parameters tend to prove that the various oxygen sites can be separated in MQ-MAS experiments. Work is in progress in the laboratory for recording ^{17}O spectra of enriched calcium phosphate phases.

Acknowledgments

Dr. D. Massiot (CRMHT) is warmly acknowledged for helpful discussions and for the access to the 750-MHz spectrometer in Orléans, France. The calculations have been performed in the IDRIS supercomputer centre of the CNRS (Project 51461).

Appendix. Supporting information

The table includes fractional atomic coordinates of $Ca_4P_2O_9$ structure after relaxation. The lattice parameters were not relaxed; $a = 7.023$ Å, $b = 11.986$ Å, $c = 9.473$ Å. The symmetry of the crystal was also constrained to be monoclinic $P1211$.

Atom	x	y	z
Ca1	0.03135	0.34484	0.89371
Ca2	0.53208	0.29963	0.89637
Ca3	0.76779	0.30400	0.53484
Ca4	0.26928	0.29958	0.25319
Ca5	0.74235	0.10865	0.25339
Ca6	0.25124	0.07842	0.01020
Ca7	0.98997	0.06827	0.63431
Ca8	0.51321	0.05225	0.58967
O1	0.73015	0.51977	0.22758
O2	0.60829	0.32156	0.28695
O3	0.95391	0.36288	0.29568
O4	0.77015	0.36447	0.05510
O5	0.28916	0.41086	0.74965
O6	0.09421	0.26407	0.62447
O7	0.45747	0.24245	0.65781
O8	0.32873	0.38221	0.48221
O9	0.21655	0.00430	0.47360
O10	0.07538	0.11672	0.26134
O11	0.42032	0.10987	0.30057
O12	0.24497	0.93066	0.22751
O13	0.58489	0.10221	1.00048
O14	0.83303	0.18754	0.84003
O15	0.71748	0.99687	0.78546
O16	0.92102	0.03030	0.01000
O17	0.26471	0.26375	0.01636
O18	0.76686	0.12650	0.48793
P1	0.76573	0.39035	0.21539
P2	0.28964	0.32559	0.62414
P3	0.23669	0.04086	0.31668
P4	0.76323	0.07675	0.91023

References

[1] D.V. Dorozhkin, M. Epple, Angew. Chem. Int. Ed. 41 (2002) 3231.
[2] M. Vallet-Regi, Chem. Eur. J. 12 (2006) 1.
[3] M. Vallet-Regi, Dalton Trans. (2006) 5211.
[4] (a) E. Fujii, M. Ohkubo, K. Tsuru, S. Hayakawa, A. Osaka, K. Kawabata, C. Bonhomme, F. Babonneau, Acta Biomater. 2 (2006) 69;
(b) S. Hayakawa, K. Ohnishi, K. Tsuru, A. Osaka, E. Fujii, K. Kawabata, F. Babonneau, C. Bonhomme, Key Eng. Mater. 309 (2006) 503;
(c) S. Hayakawa, K. Ando, K. Tsuru, A. Osaka, E. Fujii, K. Kawabata, C. Bonhomme, F. Babonneau, J. Am. Ceram. Soc. 90 (2007) 565.
[5] S. Josse, C. Faucheux, A. Soueidan, G. Grimandi, D. Massiot, B. Alonso, P. Janvier, S. Laïb, O. Gauthier, G. Daculsi, J. Guicheux, B. Bujoli, J.M. Bouler, Adv. Mater. 16 (2004) 1423.
[6] S. Josse, C. Faucheux, A. Soueidan, G. Grimandi, D. Massiot, B. Alonso, P. Janvier, S. Laïb, P. Pilet, O. Gauthier, G. Daculsi, J. Guicheux, B. Bujoli, J.-M. Bouler, Biomaterials 26 (2005) 2073.
[7] H. Roussière, G. Montavon, S. Laïb, P. Janvier, B. Alonso, F. Fayon, M. Petit, D. Massiot, J.-M. Bouler, B. Bujoli, J. Mater. Chem. 15 (2005) 3869.
[8] B. Bujoli, H. Roussière, G. Montavon, S. Laïb, P. Janvier, B. Alonso, F. Fayon, M. Petit, D. Massiot, J.-M. Bouler,

J. Guicheux, O. Gauthier, S.M. Lane, G. Nonglaton, M. Pipelier, J. Léger, D.R. Talham, C. Tellier, Prog. Solid State Chem. 34 (2006) 257.

[9] (a) W.P. Rothwell, J.S. Waugh, J.P. Yesinowski, J. Am. Chem. Soc. 102 (1980) 2637;
(b) J. Tropp, N.C. Blumenthal, J.S. Waugh, J. Am. Chem. Soc. 105 (1983) 22;
(c) P.S. Belton, R.K. Harris, P.J. Wilkes, J. Phys. Chem. Solids 49 (1988) 21;
(d) I.L. Mudrakovskii, V.P. Shmachkova, N.S. Kotsarenko, V.M. Mastikhin, J. Phys. Chem. Solids 47 (1986) 335;
(e) K. Beshah, C. Rey, M.J. Glimcher, M. Schimizu, R.G. Griffin, J. Solid State Chem. 84 (1990) 71;
(f) J.P. Yesinowski, Calcium Phosphates in Biological and Industrial Systems (1998) pp. 103–143.

[10] (a) Y. Wu, M.J. Glimcher, C. Rey, J.L. Ackerman, J. Mol. Biol. 244 (1994) 423;
(b) Y. Wu, J.L. Ackerman, E.S. Strawich, C. Rey, H.M. Kim, M.J. Glimcher, Calcif. Tissue Int. 72 (2003) 610;
(c) A. Kaflak-Hachulska, A. Samoson, W. Kolodziejski, Calcif. Tissue Int. 73 (2003) 476.

[11] J.P. Yesinowski, H. Eckert, J. Am. Chem. Soc. 109 (1987) 6274.

[12] B.C. Gerstein, R.G. Pembleton, R.C. Wilson, J. Chem. Phys. 66 (1977) 361.

[13] R.A. Santos, R.A. Wind, C.E. Bronnimann, J. Magn. Reson. B 105 (1994) 183.

[14] (a) B. Berglund, R.W. Vaughan, J. Chem. Phys. 73 (1980) 2037;
(b) G.A. Jeffrey, Y. Yeon, Acta Crystallogr. B42 (1986) 410.

[15] C.J. Pickard, F. Mauri, Phys. Rev. B 63 (2001) 245101.

[16] S.E. Ashbrook, M.E. Smith, Chem. Soc. Rev. 35 (2006) 718.

[17] B. Julian, C. Gervais, M.N. Rager, J. Maquet, E. Cordoncillo, P. Escribano, F. Babonneau, C. Sanchez, Chem. Mater. 16 (2004) 521.

[18] C. Gervais, B. Julian, E. Cordoncillo, P. Escribano, M.E. Smith, F. Babonneau, C. Sanchez, Mater. Res. Soc. Symp. Proc. (2005) 483.

[19] V. Lafond, C. Gervais, J. Maquet, D. Prochnow, F. Babonneau, P.-H. Mutin, Chem. Mater. 15 (2003) 4098.

[20] M. Zeyer, L. Montagne, V. Kostoj, G. Palavit, D. Prochnow, C. Jaeger, J. Non-Cryst. Solids (2002) 223.

[21] A. Flambard, L. Montagne, L. Delevoye, Chem. Commun. (2006) 3426.

[22] B.R. Cherry, T.M. Alam, C. Click, R.K. Brow, Z. Gan, J. Phys. Chem. B 107 (2003) 4894.

[23] L. Frydman, J.S. Harwood, J. Am. Chem. Soc. 117 (1995) 5367.

[24] A. Wong, A.P. Howes, R. Dupree, M.E. Smith, Chem. Phys. Lett. 427 (2006) 201.

[25] J.P. Perdew, K. Burke, M. Ernzerhof, Phys. Rev. Lett. 77 (1996) 3865.

[26] N. Troullier, J.L. Martins, Phys. Rev. B 43 (1991) 1993.

[27] L. Kleinman, D. Bylander, Phys. Rev. Lett. 48 (1982) 1425.

[28] N.A. Curry, D.W. Jones, J. Chem. Soc. A (1971) 3725.

[29] L.W. Schroeder, E. Prince, B. Dickens, Acta Crystallogr. B31 (1975) 9.

[30] W. Rothammel, H. Burzlaff, R. Specht, Acta Crystallogr. C45 (1989) 551.

[31] L.E. Jackson, B.M. Kariuki, M.E. Smith, J.E. Barralet, A.J. Wright, Chem. Mater. 17 (2005) 4642.

[32] B. Dickens, W.E. Brown, G.J. Kruger, J.M. Stewart, Acta Crystallogr. C29 (1973) 2046.

[33] H.J. Monkhorst, J.D. Pack, Phys. Rev. B 13 (1976) 5188.

[34] (a) M. Profeta, F. Mauri, C.J. Pickard, J. Am. Chem. Soc. 125 (2003) 541;
(b) M. Profeta, M. Benoit, F. Mauri, C.J. Pickard, J. Am. Chem. Soc. 126 (2004) 12628.

[35] D. Massiot, F. Fayon, M. Capron, I. King, S. Le Calvé, B. Alonso, J.-O. Durand, B. Bujoli, Z. Gan, G. Hoatson, Magn. Reson. Chem. 20 (2002) 70.

[36] (a) F. Fayon, G. Le Saout, L. Emsley, D. Massiot, Chem. Commun. (2002) 1702;
(b) I.J. King, F. Fayon, D. Massiot, R.K. Harris, J.S.O. Evans, Chem. Commun. (2001) 1766.

[37] F. Pourpoint, C. Gervais, L. Bonhomme-Coury, T. Azaïs, C. Coelho, F. Mauri, B. Alonso, F. Babonneau, C. Bonhomme, Appl. Magn. Reson., in press.

[38] (a) C. McMichael Rohlfing, L.C. Allen, R. Ditchfield, J. Chem. Phys. 79 (1983) 4958;
(b) T. Murakhtina, J. Heuft, E.J. Meijer, D. Sebastiani, ChemPhysChem 7 (2006) 2578.

[39] (a) F. Schönborn, H. Schmitt, H. Zimmermann, U. Haeberlen, C. Corminboeuf, G. Grossmann, T. Heine, J. Magn. Reson. 175 (2005) 52;
(b) T. Heine, C. Corminboeuf, G. Grossmann, U. Haeberlen, Angew. Chem. Int. Ed. 45 (2006) 7292.

[40] (a) N. Mifsud, B. Elena, C.J. Pickard, A. Lesage, L. Emsley, Phys. Chem. Chem. Phys. 8 (2006) 3418;
(b) J.R. Yates, S.E. Dobbins, C.J. Pickard, F. Mauri, P.Y. Ghi, R.K. Harris, Phys. Chem. Chem. Phys. 7 (2005) 1402.

[41] I. Schnell, H.W. Spiess, J. Magn. Reson. 151 (2001) 153.

[42] C. Gervais, C. Coelho, T. Azaïs, J. Maquet, G. Laurent, F. Pourpoint, C. Bonhomme, P. Florian, B. Alonso, G. Guerrero, P.-H. Mutin, F. Mauri, J Magn Reson. 187 (2007) 131.

[43] (a) M. Mehring, Principles of High Resolution NMR in Solids, Springer Verlag, 1983, pp. 236–240;
(b) U. Haeberlen Supplement, Adv. Magn. Res., Academic Press, New York, 1976;
(c) U. Haeberlen, U. Kohlschütter, J. Kempf, H.W. Spiess, H. Zimmermann, Chem. Phys. 3 (1974) 248.

[44] G. Wu, C.J. Freure, E. Verdurand, J. Am. Chem. Soc. 120 (1998) 13187.

[45] G. Wu, D. Rovnyak, P.C. Huang, R.G. Griffin, Chem. Phys. Lett. 277 (1997) 79.

[46] G.L. Turner, S.E. Chung, E.J. Oldfield, J. Magn. Reson. 64 (1985) 316.

[47] G. Wu, A. Hook, S. Dong, K. Yamada, J. Phys. Chem. A 104 (2000) 4102.

[48] Q.W. Zhang, H.M. Zhang, M.G. Usha, R.J. Wittebort, Solid State NMR 7 (1996) 147.

[49] C. Gervais, M. Profeta, V. Lafond, C. Bonhomme, T. Azaïs, H. Mutin, C.J. Pickard, F. Mauri, F. Babonneau, Magn. Reson. Chem. 42 (2004) 445.

[50] S.K. Lee, J.F. Stebbins, J. Phys. Chem. B 104 (2000) 4091.